

Interconversion between Formic Acid and H₂/CO₂ using Rhodium and Ruthenium Catalysts for CO₂ Fixation and H₂ Storage

Yuichiro Himeda,^{*,[a]} Satoru Miyazawa,^[b] and Takuji Hirose^[b]

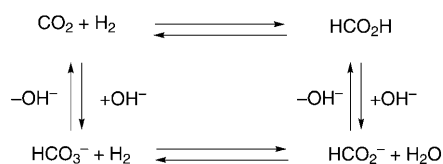
The interconversion between formic acid and H₂/CO₂ using half-sandwich rhodium and ruthenium catalysts with 4,4'-dihydroxy-2,2'-bipyridine (DHBP) was investigated. The influence of substituents of the bipyridine ligand was studied. Chemical shifts of protons in bipyridine linearly correlated with Hammett substituent constants. In the hydrogenation of CO₂/bicarbonate to formate under basic conditions, significant activations of the catalysts were caused by the electronic effect of oxyanions generated by deprotonation of the hydroxyl group. Initial turnover frequencies of the ruthenium- and rhodium-DHBP complexes increased 65- and 8-fold, respectively, compared to the

corresponding unsubstituted bipyridine complexes. In the decomposition of formic acid under acidic conditions, activity enhancement by the electronic effect of the hydroxyl group was observed for the ruthenium catalyst. The rhodium-DHBP catalyst showed high activity without CO contamination in a relatively wide pH range. Pressurized H₂ can be obtained using an autoclave reactor. The highest turnover frequency and number were obtained at 80 °C. The catalytic system provides valuable insight into the use of CO₂ as a H₂ storage material by combining CO₂ hydrogenation with formic acid decomposition.

Introduction

Among the main challenges that humans will face in the future are finding an adequate and sustainable energy supply and protecting the global environment.^[1] Promising solutions to these challenges lie in the development of a hydrogen economy, because molecular hydrogen offers advantages over fossil fuels from both environmental and economical viewpoints. However, the actual use of hydrogen is limited, mainly because of problems with its storage and delivery.^[2] Thus, the development of technologies for hydrogen storage/evolution in a reversible manner is essential.

Formic acid (which contains 4.3 wt% of H₂) and formate salt are potential H₂ storage materials because they can be handled, stored, and transported easily. The concept of using CO₂ as a H₂ storage material by the reversible reaction between formic acid and H₂/CO₂ has received renewed attention.^[3] Current research efforts are mainly devoted to the use of homogeneous catalysts for (1) the hydrogenation of CO₂/bicarbonate and (2) the decomposition of formic acid/formate (Scheme 1).



Scheme 1. Interconversion between formic acid and H₂/CO₂

Catalytic activities towards the hydrogenation of CO₂/bicarbonate for the production of formic acid/formate have been improving steadily since the early 1990s.^[4] A number of excellent Reviews on this subject have been published.^[5–9] Other

than iridium catalysts developed in our group,^[9] highly active catalysts have been achieved by using rhodium and ruthenium catalysts with phosphine ligands. Recently, Nozaki et al. reported excellent productivity when using an iridium-pincer trihydride catalyst in KOH/H₂O/THF solution at 5 MPa and 200 °C.^[10]

The decomposition of formic acid/formate for H₂ production has been studied by using a number of heterogeneous and homogeneous catalyst systems.^[11,12] In general, formic acid and formates can be decomposed via dehydrogenation/decarboxylation and dehydration/decarbonylation pathways, which are thermodynamically downhill under standard conditions. However, highly efficient and selective H₂ production under mild conditions is still required for the decomposition of formic acid. Further, when H₂ has to be used in fuel cells, CO-free (< 10 ppm) H₂ production is essential. Recently, research reported separately in two excellent papers by the groups of Beller^[13] and Laurenczy^[14] has directed renewed attention to H₂ production.^[15–19] Since then, many studies on the decomposition of formic acid/formate have been conducted, focusing mainly on ruthenium and rhodium catalysts.^[20–25] Although the concept of H₂ storage through the use of CO₂ and formic acid is well-

[a] Dr. Y. Himeda

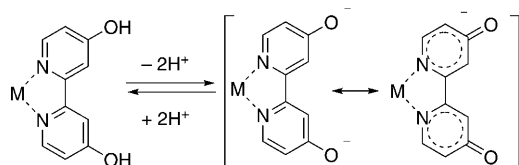
Energy Technology Research Institute
National Institute of Advanced Industrial Science and Technology
Tsukuba Central 5-2, 1-1-1 Higashi, Tsukuba, Ibaraki 305-8565 (Japan)
Fax: (+81) 29-861-6771
E-mail: himeda.y@aist.go.jp

[b] S. Miyazawa, Prof. T. Hirose

Graduate School of Science & Engineering
Saitama University, 255 Shimo-ohkubo, Sakura-ku
Saitama, Saitama 338-8570 (Japan)

known, the hydrogenation of CO₂ and the decomposition of formic acid are, except for a few studies,^[26–29] usually reported independently.

Recently, we reported that half-sandwich iridium complexes with 4,4'-dihydroxy-2,2'-bipyridine (DHBP) and 4,7-dihydroxy-1,10-phenanthroline (DHPT) ligands can act as highly efficient catalysts for the hydrogenation of CO₂/bicarbonate^[30,31] and the decomposition of formic acid.^[32] The high catalytic activity of these complexes is attributed to an electron-donating effect of the hydroxyl groups in the bipyridine ligand. In particular, the strong electron-donating effect of oxyanions generated by the deprotonation of the hydroxyl group in the DHBP ligand leads to activation that is more than 1000 times stronger than with bipyridine catalyst under basic conditions (Scheme 2).



Scheme 2. Acid–base equilibrium of DHBP complexes.

On the other hand, we have reported that during transfer hydrogenation in water the rhodium bipyridine complex decomposed formic acid to evolve H₂ gas via an undesirable side reaction.^[33,34] We then reported a turnover frequency (TOF) of 238 h⁻¹ for the decomposition of formic acid using a rhodium complex at 40 °C and pH 3.5.^[31] However, we have reported only the preliminary results obtained using rhodium and ruthenium catalysts with the DHBP ligand,^[30] although a number of rhodium and ruthenium catalysts are known to be effective in the hydrogenation of CO₂/bicarbonate and decomposition of formic acid.

In this study, we elucidate the electronic substituent effects of rhodium and ruthenium catalysts, and make a comparison with those of the iridium catalyst, in the hydrogenation of CO₂/bicarbonate under basic conditions and decomposition of formic acid under acidic conditions. We also investigate the influence of the central metal on the activation energies of the catalysts.

Results and Discussion

Syntheses and properties

DHBP aqua complexes **1–3** were prepared according to literature procedures.^[35] The chemical shifts of these complexes were examined under acidic and basic conditions in D₂O (Table 1). The addition of KOD caused upfield shifts in the ¹H NMR signals of the 3,3' (0.54–0.61 ppm), 5,5' (0.53–0.64 ppm), and 6,6' protons (0.48–0.55 ppm), and downfield shifts in the ¹³C NMR signals of the 4,4'-carbons (8.24–8.50 ppm). These shifts can be attributed to an increase in the electronic density by the deprotonation of the hydroxyl groups in the bipyridine ligand. In a similar manner, significant

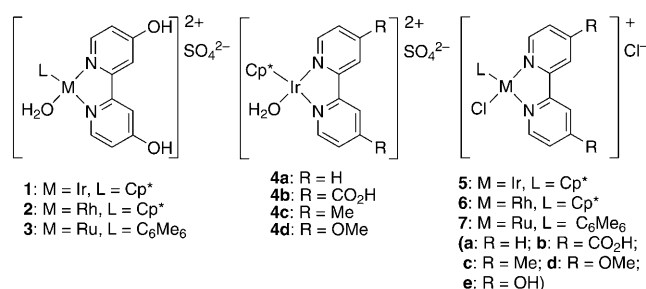


Table 1. Chemical shifts (ppm) for DHBP complexes (**1–3**) in D₂O.

Signal	Complex 1		Complex 2		Complex 3	
	D ₂ O	KOD	D ₂ O	KOD	D ₂ O	KOD
3,3'-H	7.24	6.63	7.24	6.69	7.18	6.64
5,5'-H	7.77	7.13	7.69	7.14	7.59	7.06
6,6'-H	8.77	8.25	8.76	8.28	8.74	8.19
4,4'-C	170.37	178.61	170.34	178.83	170.18	178.68

changes (3,3'-H: 0.38, 5,5'-H: 0.34, and 6,6'-H: 0.33 ppm) were observed in complex **4b** (R=CO₂H). On the other hand, slight upfield shifts of the aromatic protons in **4a** (R=H; up to 0.13 ppm), **4c** (R=Me; up to 0.11 ppm), and **4d** (R=OMe; up to 0.12 ppm) were observed because of the acid–base equilibrium of the aqua ligand.^[36]

The electronic substituent effects on the chemical shifts of the complexes with the disubstituted bipyridine were investigated under acidic and basic conditions. The Hammett substituent constant (σ_p^+) values for the hydroxyl and carboxylic acid groups under acidic conditions are –0.92 and 0.42, respectively. On the other hand, under basic conditions the values for these complexes are –2.30 and –0.02, corresponding to oxyanion (O⁻) and carboxylate (CO₂⁻), respectively. According to this interpretation, the Hammett plots for the iridium, rhodium, and ruthenium series showed a good correlation (Figure 1).

Hydrogenation of CO₂/bicarbonate under basic conditions

In a previous paper, we reported that iridium DHBP complex **1** is a highly efficient catalyst in the hydrogenation of CO₂/bicarbonate in water.^[30] In addition, we observed good correlation between the σ_p^+ values and the initial TOFs of the 4,4'-disubstituted-2,2'-bipyridine complexes. However, we reported only the preliminary results for the hydrogenation of CO₂/bicarbonate using rhodium and ruthenium catalysts.

Electronic substituent effects on the hydrogenation of CO₂/bicarbonate using the iridium (**5**), rhodium (**6**), and ruthenium series (**7**) were investigated in a 1 M KOH solution at 80 °C and 1 MPa H₂/CO₂ (1:1). The Hammett plot for the iridium series indicates good correlation between the initial TOFs and the σ_p^+ values and a high *p*-value of –1.3; these results are consistent with previous results obtained at 4 MPa (Figure 2).^[30] The initial TOF of DHBP complex **5e** was 1100 times higher than that of bipyridine complex **5a** (Table 2, entries 1 and 4). The final con-

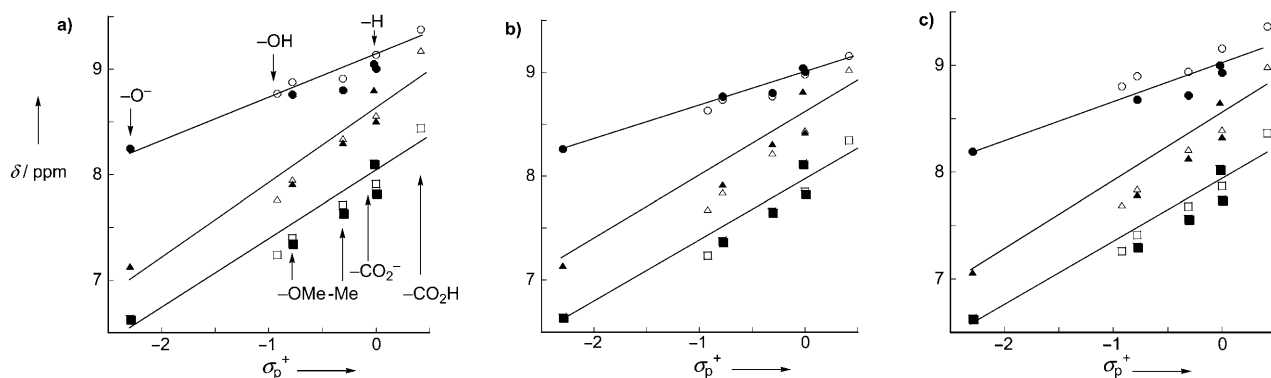


Figure 1. Correlation between the Hammett substituent constant (σ_p^+) and the chemical shifts of 3,3'-H (open squares: D₂O, closed squares: KOD/D₂O), 5,5'-H (open triangles: D₂O, closed triangles: KOD/D₂O), and 6,6'-H (open circles: D₂O, closed circles: KOD/D₂O) for (a) iridium complexes (**1** and **4a–d**), (b) rhodium complexes **6a–e**, and (c) ruthenium complexes **7a–e**.

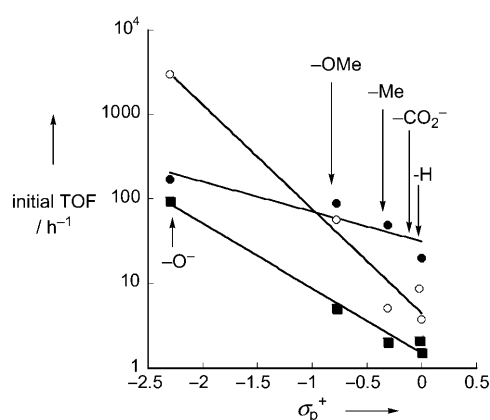


Figure 2. Correlation between initial TOFs and σ_p^+ values of substituent (R) in hydrogenation of CO₂ at 1 MPa (H₂/CO₂ = 1:1) in 1 M aqueous KOH solution at 80 °C using (a) iridium catalysts **5a–e** (0.1 mM) (open circles), (b) rhodium catalysts **6a–e** (0.1 mM) (closed circles), and (c) ruthenium catalysts **6a–e** (0.2 mM) (closed squares).

Table 2. Hydrogenation of CO ₂ /bicarbonate. ^[a]							
Entry	Catalyst	Amount [mM]	Time [h]	Temp. [°C]	Initial TOF [h ⁻¹]	TON	Final conc. of formate [M]
1	5e	0.02	30	80	5100	11 000	0.22
2	6e	0.1	30	80	160	1200	0.12
3	7e	0.1	100	80	92	5400	0.54
4	5a	0.2	30	80	4.5	120	0.023
5	6a	0.2	30	80	20	190	0.037
6	7a	0.2	30	80	1.4	45	0.009
7	7e	0.2	32	100	300	2900	0.58

[a] The reaction was carried out in a degassed 1 M KOH solution (10 mL) at 1 MPa of H₂/CO₂ (1:1). TON: turn-over number.

centration of formate generated at 1 MPa (0.22 M) was lower than that at 4 MPa (0.80 M).^[30] The rhodium-bipyridine catalyst **6a** exhibited the highest catalytic activity among the iridium- and ruthenium-bipyridine catalysts (entries 4–6). However, the initial TOF of DHBP complex **6e** was 8 times higher than that

of bipyridine complex **6a** (entries 2 and 5). The degree of catalytic activation caused by the electronic substituent effect was not strong in the case of the rhodium series. The rate of formate generation decreased considerably after 8 h and the final concentration of formate was only 0.12 M, probably because the catalyst degraded. In the case of the ruthenium series too, the Hammett plot showed a good correlation between the initial TOFs and the σ_p^+ values, although the catalytic performance was moderate. The initial TOF of DHBP complex **7e** was 65 times higher than that of bipyridine complex **7a** (entries 3 and 6). The rate of formate generation was almost constant until 50 h and the final formate concentration was 0.54 M after 100 h. This suggests that the ruthenium catalyst is relatively stable. At 100 °C, formate was generated at a higher reaction rate without significant degradation of the catalyst (entry 7). All of the reactions involving rhodium- and ruthenium-DHBP catalysts remained soluble during the course of the reaction.^[37]

From the Arrhenius plot of the temperature dependence of the initial TOF, the apparent activation energies of the iridium- (**5e**), rhodium- (**6e**), and ruthenium-DHBP catalysts (**7e**) were found to be 58, 72, and 78 kJ mol⁻¹, respectively (Figure 3). The activation energies required for the hydrogenation of bicarbonate in water using [RhCl(PPMS)₃], [RuCl₂(PTA)₄], and [(C₆H₆)RuCl₂]₂+4 PTA (1,3,5-triaza-7-phosphaadamantane) are 36,^[38] 86,^[39] and 126 kJ mol⁻¹,^[40] respectively. It seems likely that the difference in rate-determining steps in the hydrogenation reaction reflected the difference in the activation energies of the catalysts.^[36]

The activity enhancement of the rhodium and ruthenium catalysts by the electronic substituent effect of the oxyanions was confirmed on the basis of the correlation between the initial TOF and the σ_p^+ values of the substituents. Under aqueous

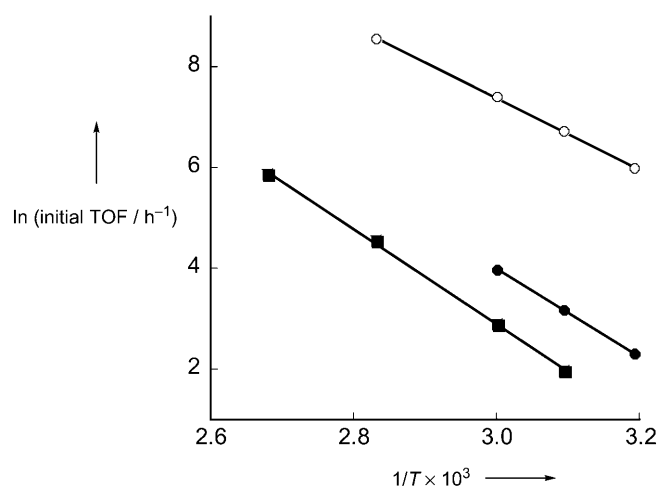


Figure 3. Arrhenius plots of initial TOF for hydrogenation of CO₂ using **5e** (open circles), **6e** (closed circles), and **7e** (closed squares) (0.1–0.05 mM) at 1 MPa (H₂/CO₂ = 1:1).

conditions, the ruthenium-DHBP catalyst **3** showed higher efficiency than the other ruthenium catalysts used in earlier studies.

Decomposition of formic acid/formate under acidic conditions

In our previous study,^[32] iridium-DHBP complex **1** acted as a highly efficient and selective catalyst for the decomposition of formic acid with complete conversion of formic acid in water (Table 3, entry 1). On the other hand, the rhodium and ruthenium catalysts showed moderate to poor performances under the same conditions (entries 2 and 3).

When using the series of the rhodium and ruthenium catalysts gas evolution was observed. The amount of an evolved gas increased linearly at time following a brief induction period at the beginning of the reaction. Because DHBP cata-

lysts are strongly dependent on pH, the pH values of the reaction solution were optimized for **2** and **3**. The TOFs and concentration of residual formate at various pH values of 1 M HCO₂H/HCO₂Na solution are shown in Figure 4. The initial TOFs of **2** exceeded 1200 h⁻¹ in the pH range 2.5–4.0 (Table 3,

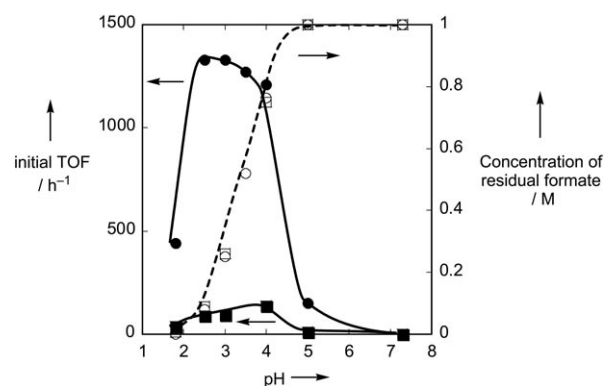


Figure 4. pH dependence of gas evolution at 60 °C in 1 M HCO₂H/HCO₂Na (10 mL) at various pH values. (a) Initial TOF (closed circles) and (b) concentration of residual formate (open circles) using **2** (0.2–0.4 mM), (c) initial TOF (closed squares) and (d) concentration of residual formate (open squares) using **3** (0.5–1.0 mM).

entry 4), while the maximum TOF of catalyst **1** was attained in the case of an aqueous formic acid solution (pH 1.8). The TOFs of **3** were moderate (maximum TOF 140 h⁻¹ at pH 4.0, entry 5). The TOFs of **2** and **3** dropped significantly in pure formic acid solution and at pH values above 5. The trends of TOFs of **2** and **3** were different from that of **1**.

On the other hand, the trends of the conversions of formic acid of **2** and **3** were similar to that of **1**. At the end of the reaction in pure formic acid solution, no formic acid was detected (Table 3, entries 2 and 3). An increase of the pH caused an increase of the concentration of the residual formate in the reaction solution. Moreover, negligible gas evolution was detected in the sodium formate solution. It was clear that formic acid had decomposed whereas formate, necessary for achieving high reaction efficiency, had not decomposed. In addition, similar to the reactions using **1**,^[32] CO was not detected in the evolved gas for all the reactions (gas chromatography using a flame ionization detector equipped with a methanizer).

Electronic substituent effects were investigated by using the series of rhodium and ruthenium catalysts **6a–e** and **7a–e**, respectively, at pH 3.0. All the catalysts of the rhodium series exhibited high initial TOFs (Table 3, entries 6–9). However, the catalytic

Table 3. Decomposition of formic acid/formate. ^[a]								
Entry	Catalyst	Amount [mM]	Solution	Time [h]	Temp. [°C]	Initial TOF [h ⁻¹]	TON	Conversion ^[b] [%]
1 ^[c]	1	0.2	HCO ₂ H	5	60	2400	5000	100
2	2	0.4	HCO ₂ H	24	60	440	5000	100
3	3	1.0	HCO ₂ H	48	60	36	5000	>99
4	2	0.2	pH 2.5	7	60	1340	4600	92
5	3	0.5	pH 4.0	9	60	140	500	25
6	6a	0.2	pH 3.0	6	60	1230	3700	73
7	6c	0.2	pH 3.0	5	60	1350	3700	74
8	6d	0.2	pH 3.0	6	60	1270	3800	75
9	6e	0.2	pH 3.0	5	60	1340	3800	75
10	7e	0.5	pH 3.0	24	60	94	3700	74
11	2	0.1	pH 2.5	2.5	80	7900	9300	93
12	3	0.5	pH 3.0	5	80	720	1600	80
13 ^[d]	2	–	–	50	80	7700	83 000	75

[a] The reaction was carried out in a degassed 1 M formic acid/formate solution (10 mL) until gas evolution ceased. [b] Conversion was calculated by the residual formate. [c] See Ref. [32]. [d] The reaction was carried out using **2** (2 μmol) in a degassed 4 M formic acid solution (50 mL) and 4 M sodium formate solution (5 mL).

activity of **6b** significantly decreased after 1 h, probably because of catalyst degradation, although an initial TOF of ca. 900 was observed. These results show that the series of rhodium catalysts were not influenced by electronic substituent effects. In the case of the rhodium series, the rate-determining step may be different from that of the iridium series. In the case of the ruthenium catalyst series, the initial TOF of **7e** (entry 10) was approximately 2.9 times that of unsubstituted analogue **7a**. On the other hand, the activity for **7b** was less, because of the electron-withdrawing effect of carboxyl group ($\sigma_p^+ = 0.42$). The TOF values for the series of ruthenium catalysts show a good correlation with the Hammett substituent constants (Figure 5).

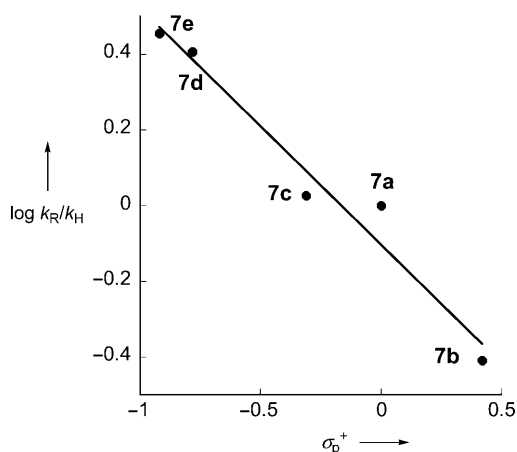


Figure 5. Hammett plot for initial TOFs vs. σ_p^+ values of substituent (R) in ruthenium catalysts **7a–e** (0.5–1.0 mM) at 60 °C in 1 M aqueous HCO₂H/HCO₂Na solution (10 mL) at pH 3.0.

The temperature dependence of the TOFs was investigated also. In the case of **2**, the highest TOF of 7900 h⁻¹ was obtained at 80 °C and pH 2.5, with a conversion rate of 93% (entry 11). These values are comparable to those of iridium analogue **1**. For **3**, a satisfactory TOF of 720 h⁻¹ was obtained at 80 °C (Table 3, entry 12). Further, in the case of **2** (2 μmol), a highest turnover number (TON) of 83 000 was obtained in a 4 M HCO₂H/HCO₂Na solution at 80 °C after 50 h (entry 13). Figure 6 shows the Arrhenius plots for **1**,^[32] **2**, and **3**. The apparent activation energies of **2** and **3** are 93 kJ mol⁻¹ and 96 kJ mol⁻¹, respectively, which are higher than that of **1** (76 kJ mol⁻¹).^[32]

Pressurized gas supply will be essential in practical applications (e.g., for separation and filling of gas). A spontaneous increase of the gas pressure has been observed in a closed system, similar to the iridium catalyst.^[32] When the reaction catalyzed by **2** in a 2 M HCO₂H/HCO₂Na (95:5) solution was carried out in an autoclave, the pressure of the evolved gas exceeded 5 MPa after 4 h, and 92 mm of formate (4.6%) remained at the end of the reaction (Figure 7). Thus, the gas pressure in the system did not inhibit the decomposition of formic acid.

Highly efficient H₂ evolution was achieved in water using **2** by the adjusting the reaction conditions. The excellent results obtained in the case of **2** were comparable to those obtained

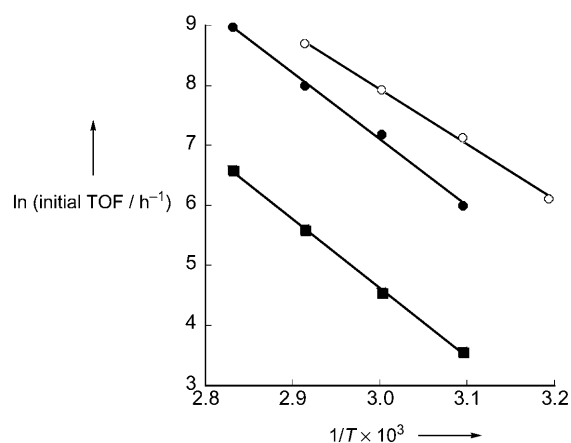


Figure 6. Arrhenius plots of initial TOFs for decomposition of formic acid using (a) **1** (0.2 mM) in 2 M aqueous HCO₂H solution (open circles), (b) **2** (0.1–0.2 mM) in 1 M aqueous HCO₂H/HCO₂Na solution at pH 2.5 (closed circles), and (c) **3** (0.5–1.0 mM) in 1 M aqueous HCO₂H/HCO₂Na solution at pH 3.0 (closed squares).

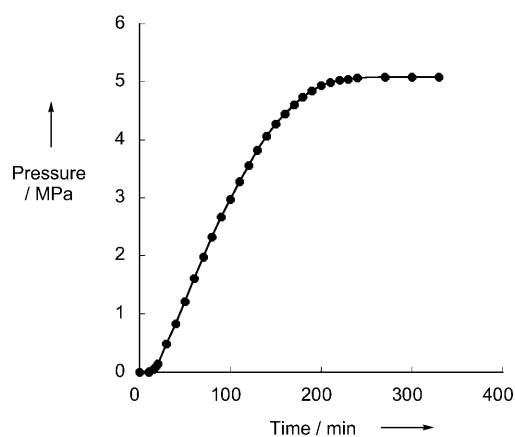


Figure 7. Time course of pressure using **2** (0.2 mM) at 80 °C in 2 M HCO₂H/HCO₂Na (95:5) solution (10 mL) in glass autoclave.

in the case of **1**, although a small amount of formate salt was required for ensuring high reaction efficiency in the former case. CO-free H₂ was produced with a high TOF (up to 7900 h⁻¹), high TON (up to 83 000), and conversion of formic acid (up to 100%). In addition, pressurized H₂ can be obtained in a closed reactor. The electronic substituent effects and activation energies for **2** and **3** provide valuable mechanistic insight.

Conclusions

The interconversion between formic acid and H₂/CO₂ using rhodium and ruthenium catalysts with DHBP in water is demonstrated. Catalytic activations caused by an electronic substituent effect of the oxyanions in the rhodium and ruthenium catalysts with DHBP ligand in the hydrogenation of CO₂/bicarbonate are observed under basic conditions. Relatively high TONs and TOFs are obtained using the ruthenium-DHBP catalyst. In addition, an electronic substituent effect in the decom-

position of formic acid/formate under acidic conditions is observed in the case of the ruthenium catalyst. The rhodium-DHBP catalyst shows efficient catalytic performance without CO contamination in the pH range 2.5–4.0, although a small amount of formate is required. In addition, pressurized H₂ is obtained by using an autoclave reactor. We believe that the DHBP ligand plays an important role in both the reactions: hydrogenation of CO₂ and decomposition of formic acid.

The DHBP catalyst system offers several excellent properties for practical use in a H₂ storage system. The aqueous reaction without use of organic additives will be essential from an economical and ecological point of view. The selection of the direction of reactions (i.e., formation/decomposition of formic acid) by adjusting the pH using the same catalyst offers the possibility of H₂ storage. Further investigations on the reversibility of storage and evolution of H₂ in the same vessel are in progress. Furthermore, it should be noted that H₂ generated from renewable sources is required for large-scale applications, although CO₂ fixation using rhodium and ruthenium catalysts may be employed for effective H₂ storage.

Experimental Section

All manipulations were carried out under an argon atmosphere using standard Schlenk techniques or in a glovebox. All aqueous solutions were degassed prior to use. ¹H NMR and ¹³C NMR spectra were recorded on a Varian INOVA 400 spectrometer using sodium 3-(trimethylsilyl)-1-propanesulfonate (DSS) and tetramethylsilane (TMS) as an internal standard. ESI-MS was measured with a Micro-mass QUATTRO II mass spectrometer. Elemental analyses were carried out on an Eager 200 instrument. FTIR spectra were recorded on a Perkin-Elmer Spectrum One spectrometer. pH values were measured on an Orion Model 290 A pH meter with a glass electrode after calibration to standard buffer solutions. The gas samples, which were obtained at various intervals with a gastight syringe through a septum, were analyzed for H₂ with a TCD (thermal conductivity detector) using an activated carbon 60/80. In case of CO₂, the samples were analyzed with an FID equipped with a methaniser using a Porapak Q 80/100 at 50 °C, on a GL Science GC390 gas chromatograph. The formate concentrations were monitored by an HPLC on an anion-exclusion column (Tosoh TSKgel SCX(H⁺)) with an aqueous phosphate solution (20 mM) as an eluent and a UV detector (λ = 210 nm).^[41] Research grade CO₂ (>99.999%) and H₂ (>99.9999%) were used. [Cp*⁺RhCl₂]₂, [Cp*⁺IrCl₂]₂, [(C₆Me₆)RuCl₂]₂, 4,4'-dicarboxy-2,2'-bipyridine, 4,4'-dimethyl-2,2'-bipyridine, and 4,4'-dimethoxy-2,2'-bipyridine were commercially available from either Aldrich, Tokyo Kasei, or Strem. The 4,4'-dihydroxy-2,2'-bipyridine,^[42] **1–3**, **4a–d**,^[35] **5a–e**, **6a**, **6e**, **7a**, **7e**,^[30] and **6b,c**^[43] were prepared according to literature procedures.

Preparation of rhodium complex with 4,4'-dimethoxy-2,2'-bipyridine (6d): A methanol solution (20 mL) of [Cp*⁺RhCl₂]₂ (309 mg, 0.50 mmol) and 4,4'-dimethoxy-2,2'-bipyridine (220 mg, 0.51 mmol) was stirred at RT for 12 h. The solvent was removed in vacuo and the residue was dissolved in a minimum amount of acetonitrile. Addition of ethyl acetate gave a pale yellow solid **6d** (510 mg, 97%), which was collected, washed with ether, and dried in vacuo. An analytical sample was obtained by recrystallization from CH₃CN/AcOEt: ¹H NMR ([D₆]DMSO): δ = 8.73 (d, *J* = 6.6 Hz, 2H), 8.29 (d, *J* = 2.7 Hz, 2H), 7.42 (dd, *J* = 6.6, 2.7 Hz, 2H), 4.07 (s, 6H),

1.64 ppm (s, 15H); ¹³C NMR ([D₆]DMSO): δ = 168.57, 155.96, 153.50, 114.82, 110.89, 96.78 (d, *J*_{Rh–C} = 4.0 Hz), 57.59, 8.97 ppm; IR (KBr), $\tilde{\nu}$ = 1615, 1560, 1493, 1338, 1252, 1233; ESIMS: *m/z* 489 [M–Cl]⁺; Anal. calcd for C₂₂H₂₇Cl₂N₂O₂Rh: C 50.30, H 5.18, N 5.33, found: C 50.05, H 5.18, N 5.22.

Preparation of ruthenium complex with 4,4'-dicarboxy-2,2'-bipyridine (7b): A DMF solution (30 mL) of [(C₆Me₆)RuCl₂]₂ (334 mg, 0.50 mmol) and 4,4'-dicarboxy-2,2'-bipyridine (244 mg, 1.00 mmol) was stirred at 40 °C for 12 h. The reaction solution was filtered off. The volume of the filtrate was reduced to ~5 mL in vacuo and ethyl acetate was added to precipitate **7b** as a pale yellow solid (503 mg, 87%). An analytical sample was obtained by chromatography on a Sephadex LH-20 (Pharmacia Fine Chemicals) column: ¹H NMR ([D₆]DMSO): δ = 8.99 (d, *J* = 5.7 Hz, 2H), 8.64 (d, *J* = 1.6 Hz, 2H), 7.68 (dd, *J* = 1.6, 5.7 Hz, 2H), 2.05 (s, 18H); ¹H NMR (KOD/D₂O): δ = 9.00 (d, *J* = 6.0 Hz, 2H), 8.65 (d, *J* = 1.6 Hz, 2H), 8.04 (dd, *J* = 1.6, 5.8 Hz, 2H), 2.06 ppm (s, 18H); ¹³C NMR (KOD/D₂O): δ = 173.3, 158.1, 156.1, 150.1, 129.0, 124.6, 57.0, 6.17 ppm; ESIMS; *m/z* 541 [M–Cl]⁺; Anal. calcd for C₂₄H₂₆Cl₂N₂O₄Ru·CH₃OH: C 49.19, H 4.95, N 4.59, found: C 49.23, H 4.76, N 4.32.

Preparation of ruthenium complex with 4,4'-dimethyl-2,2'-bipyridine (7c): In the same manner as described for the preparation of **6d**, [(C₆Me₆)RuCl₂]₂ (500 mg, 0.75 mmol) was treated with 4,4'-dimethyl-2,2'-bipyridine (276 mg, 1.50 mmol) to give **7c** as an orange precipitate (662 mg, 80%): ¹H NMR ([D₆]DMSO): δ = 8.75 (d, *J* = 5.9 Hz, 2H), 8.49 (bs, 2H), 7.68 (dd, *J* = 1.0, 5.9 Hz, 2H), 2.57 (s, 6H), 2.02 ppm (s, 18H); ¹³C NMR ([D₆]DMSO): δ = 154.15, 153.11, 151.75, 128.60, 124.24, 95.32, 20.88, 15.33 ppm; IR (KBr) $\tilde{\nu}$ = 1614, 1482, 1444, 1389, 1010, 837; ESIMS *m/z* 483 [M–Cl]⁺; Anal. calcd for C₂₄H₃₀Cl₂N₂Ru·3/2H₂O: C 52.84, H 6.10, N 5.14, found: C 52.55, H 6.14, N 5.02.

Preparation of ruthenium complex with 4,4'-dimethoxy-2,2'-bipyridine (7d): In the same manner as described for the preparation of **6d**, [(C₆Me₆)RuCl₂]₂ (335 mg, 0.50 mmol) was treated with 4,4'-dimethoxy-2,2'-bipyridine (219 mg, 1.01 mmol) to give **7d** as an orange precipitate (510 mg, 93%): ¹H NMR ([D₆]DMSO): δ = 8.66 (d, *J* = 6.6 Hz, 2H), 8.24 (d, *J* = 2.7 Hz, 2H), 7.37 (dd, *J* = 6.6, 2.7 Hz, 2H), 4.05 (s, 6H), 2.02 ppm (s, 18H); ¹³C NMR ([D₆]DMSO): δ = 167.88, 155.84, 154.49, 114.18, 111.30, 94.78, 57.26, 15.34 ppm; IR (KBr) $\tilde{\nu}$ = 1610, 1492, 1416, 1340, 1280, 1230, 1044; ESIMS *m/z* 515 [M–Cl]⁺; Anal. calcd for C₂₄H₃₂Cl₂N₂O₂Ru·3/2H₂O: C 49.91, H 5.76, N 4.85, found: C 50.29, H 5.53, N 4.87.

Procedure for catalytic hydrogenation of CO₂/bicarbonate: A degassed aqueous 1 M KOH solution (50 mL) of the complex was saturated with CO₂ in a 100 mL stainless steel reactor equipped with a sampling device. The reactor was heated and then repressurized with 1 MPa (CO₂:H₂ = 1:1). At appropriate intervals, samples were removed and analyzed by HPLC. The initial TOF was calculated using nonlinear least-squares fitting of the experimental data obtained from the initial part of the reaction.^[44]

Procedure for catalytic decomposition of formic acid/formate: Typically, a 20 mM solution of catalyst (100 μL, 2 μmol) was added to a deaerated aqueous HCO₂H/HCO₂Na solution, and the mixture was stirred at the desired temperature. The volume of gas evolution was determined by a gas meter (Shinagawa Corp., W-NK-05). The initial TOF was calculated using linear least-squares fitting of the experimental data obtained from the initial part of the reaction with the exception of the brief induction period.

Acknowledgements

We are grateful to the Ministry of Economy, Trade, and Industry for providing financial support.

Keywords: carbon dioxide fixation · formic acid · hydrogen storage · rhodium · ruthenium

- [1] N. Armaroli, V. Balzani, *Angew. Chem.* **2007**, *119*, 52–67; *Angew. Chem. Int. Ed.* **2007**, *46*, 52–66.
- [2] U. Eberle, M. Felderhoff, F. Schuth, *Angew. Chem.* **2009**, *121*, 6732–6757; *Angew. Chem. Int. Ed.* **2009**, *48*, 6608–6630.
- [3] R. Williams, R. S. Crandall, A. Bloom, *Appl. Phys. Lett.* **1978**, *33*, 381–383.
- [4] C. Federsel, R. Jackstell, M. Beller, *Angew. Chem.* **2010**, *122*, 6392–6395; *Angew. Chem. Int. Ed.* **2010**, *49*, 6254–6257.
- [5] W. Leitner, *Angew. Chem.* **1995**, *107*, 2391–2405; *Angew. Chem. Int. Ed. Engl.* **1995**, *34*, 2207–2221.
- [6] P. G. Jessop, T. Ikariya, R. Noyori, *Chem. Rev.* **1995**, *95*, 259–272.
- [7] P. G. Jessop, F. Joó, C. C. Tai, *Coord. Chem. Rev.* **2004**, *248*, 2425–2442.
- [8] P. G. Jessop, *Handbook of Homogeneous Hydrogenation*, Vol. 1 (Eds.: J. G. de Vries, C. J. Elsevier), Wiley-VCH, Weinheim, **2007**, pp. 489–511.
- [9] Y. Himeda, *Eur. J. Inorg. Chem.* **2007**, 3927–3941.
- [10] R. Tanaka, M. Yamashita, K. Nozaki, *J. Am. Chem. Soc.* **2009**, *131*, 14168–14169.
- [11] B. Loges, A. Boddien, F. Gartner, H. Junge, M. Beller, *Top. Catal.* **2010**, *53*, 902–914.
- [12] T. C. Johnson, D. J. Morris, M. Wills, *Chem. Soc. Rev.* **2010**, *39*, 81–88.
- [13] B. Loges, A. Boddien, H. Junge, M. Beller, *Angew. Chem.* **2008**, *120*, 4026–4029; *Angew. Chem. Int. Ed.* **2008**, *47*, 3962–3965.
- [14] C. Fellay, P. J. Dyson, G. Laurenczy, *Angew. Chem.* **2008**, *120*, 4030–4032; *Angew. Chem. Int. Ed.* **2008**, *47*, 3966–3968.
- [15] H. Junge, A. Boddien, F. Capitta, B. Loges, J. R. Noyes, S. Gladiali, M. Beller, *Tetrahedron Lett.* **2009**, *50*, 1603–1606.
- [16] A. Boddien, B. Loges, H. Junge, F. Gartner, J. R. Noyes, M. Beller, *Adv. Synth. Catal.* **2009**, *351*, 2517–2520.
- [17] A. Boddien, B. Loges, H. Junge, M. Beller, *ChemSusChem* **2008**, *1*, 751–758.
- [18] W. J. Gan, P. J. Dyson, G. Laurenczy, *React. Kinet. Catal. Lett.* **2009**, *98*, 205–213.
- [19] C. Fellay, N. Yan, P. J. Dyson, G. Laurenczy, *Chem. Eur. J.* **2009**, *15*, 3752–3760.
- [20] D. J. Morris, G. J. Clarkson, M. Wills, *Organometallics* **2009**, *28*, 4133–4140.
- [21] X. L. Li, X. Y. Ma, F. Shi, Y. Q. Deng, *ChemSusChem* **2010**, *3*, 71–74.
- [22] A. Majewski, D. J. Morris, K. Kendall, M. Wills, *ChemSusChem* **2010**, *3*, 431–434.
- [23] A. Boddien, B. Loges, F. Gartner, C. Torborg, K. Fumino, H. Junge, R. Ludwig, M. Beller, *J. Am. Chem. Soc.* **2010**, *132*, 8924–8934.
- [24] S. Fukuzumi, T. Kobayashi, T. Suenobu, *J. Am. Chem. Soc.* **2010**, *132*, 1496–1497.
- [25] S. Fukuzumi, T. Kobayashi, T. Suenobu, *ChemSusChem* **2008**, *1*, 827–834.
- [26] M. L. Man, Z. Y. Zhou, S. M. Ng, C. P. Lau, *Dalton Trans.* **2003**, 3727–3735.
- [27] Y. Gao, J. K. Kuncheria, H. A. Jenkins, R. J. Puddephatt, G. P. A. Yap, *J. Chem. Soc. Dalton Trans.* **2000**, 3212–3217.
- [28] W. Leitner, E. Dinjus, F. Gassner, *J. Organomet. Chem.* **1994**, *475*, 257–266.
- [29] D. Preti, S. Squarcialupi, G. Fachinetti, *Angew. Chem.* **2010**, *122*, 2635–2638; *Angew. Chem. Int. Ed.* **2010**, *49*, 2581–2584.
- [30] Y. Himeda, N. Onozawa-Komatsuzaki, H. Sugihara, K. Kasuga, *Organometallics* **2007**, *26*, 702–712.
- [31] Y. Himeda, N. Onozawa-Komatsuzaki, H. Sugihara, H. Arakawa, K. Kasuga, *Organometallics* **2004**, *23*, 1480–1483.
- [32] Y. Himeda, *Green Chem.* **2009**, *11*, 2018–2022.
- [33] Y. Himeda, N. Onozawa-Komatsuzaki, H. Sugihara, H. Arakawa, K. Kasuga, *J. Mol. Catal. A: Chem.* **2003**, *195*, 95–100.
- [34] Y. Himeda, N. Onozawa-Komatsuzaki, H. Sugihara, H. Arakawa, K. Kasuga, *The 50th Symposium on Coordination Chemistry of Japan*, Japan Society of Coordination Chemistry, Kusatsu, **2000**, 1P3K01.
- [35] a) Y. Himeda, N. Onozawa-Komatsuzaki, S. Miyazawa, H. Sugihara, T. Hirose, K. Kasuga, *Chem. Eur. J.* **2008**, *14*, 11076–11081; b) Y. Himeda, S. Miyazawa, N. Onozawa-Komatsuzaki, T. Hirose, K. Kasuga, *Dalton Trans.* **2009**, 6286–6288.
- [36] S. Ogo, R. Kabe, H. Hayashi, R. Harada, S. Fukuzumi, *Dalton Trans.* **2006**, 4657–4663.
- [37] Y. Himeda, N. Onozawa-Komatsuzaki, H. Sugihara, K. Kasuga, *J. Am. Chem. Soc.* **2005**, *127*, 13118–13119.
- [38] A. Katho, Z. Opre, G. Laurenczy, F. Joó, *J. Mol. Catal. A: Chem.* **2003**, *204*, 143–148.
- [39] G. Laurenczy, F. Joó, L. Nadasdi, *Inorg. Chem.* **2000**, *39*, 5083–5088.
- [40] H. Horváth, G. Laurenczy, A. Katho, *J. Organomet. Chem.* **2004**, *689*, 1036–1045.
- [41] N. Komatsuzaki, Y. Himeda, T. Hirose, H. Sugihara, K. Kasuga, *Bull. Chem. Soc. Jpn.* **1999**, *72*, 725–731.
- [42] Y. R. Hong, C. B. Gorman, *J. Org. Chem.* **2003**, *68*, 9019–9025.
- [43] U. Kölle, B. S. Kang, P. Infelta, P. Comte, M. Gratzel, *Chem. Ber.* **1989**, *122*, 1869–1880.
- [44] K. Kudo, N. Sugita, Y. Takezaki, *Nippon Kagaku Kaishi* **1977**, 302–309.

Received: October 1, 2010

Revised: December 6, 2010

Published online on January 26, 2011